

## Motivation

### • keV-particle impact → atomic collision cascade

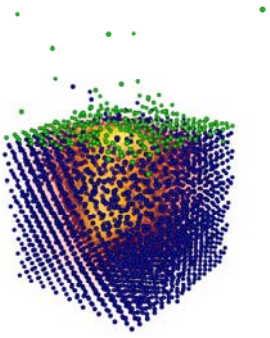
- elastic collisions
- electronic excitation
- particle emission

### • kinetic excitation

- hot electron-hole pair generation
- ionization & excitation of sputtered particles
- kinetic electron emission

### • model description

- electronic excitation mechanisms
- excitation energy transport
- secondary ion formation mechanisms
- model for kinetic electron emission

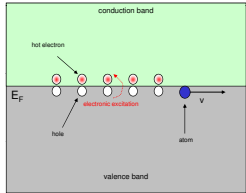


model system: Ag → Ag (111)

## Electronic Excitation Model

### Excitation Mechanisms

#### • electronic friction



- direct atom-electron collisions
- electronic stopping (Fig. 1)
- velocity-proportional friction force
- Fermi-like excitation spectrum →  $T_e$  (Fig. 2)

→ total excitation energy source rate:

$$\frac{dE(\mathbf{r}, t)}{dt} = A \sum_i E_i(\mathbf{r}, t) \cdot \delta(\mathbf{r}_i - \mathbf{r}) = A E_i(\mathbf{r}, t)$$

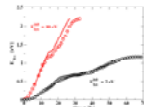


Fig. 1: Energy  $E_{eh}$  dissipated into electron-hole pair excitation as a function of time for different kinetic energies of a hot electron impinging onto an Ag(111) surface. Results from TDFFT simulations are compared to predictions from the Lindhard theory of electronic stopping.

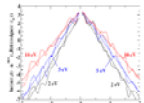


Fig. 2: Excitation spectrum for holes and electrons in the Ag simulation volume.

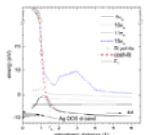
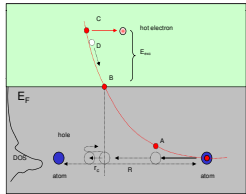


Fig. 3: Ab-initio HF-calculation of MO energies for interatomic distances corresponding to a close-packed structure of the Ag-Ag atoms. The red dashed line constitutes the diabatic MO level generally constructed from the diabatic ones.

#### • electron promotion



- close atom-atom collisions
- quasi-molecular orbital formation
- „diabatic“ curve crossing (Fig. 3)
- electron promotion above Fermi level
- resonant autoionizing transitions into free conduction band states
- generation of hot electrons above  $E_F$

## Transport

#### • free electron gas model

- nonlinear diffusive transport of excitation energy
- crucial parameter:  $D_e$  „excitation energy diffusivity“
- $D$  may vary in space and time as a function of

- lattice temperature  $T_l$
- electron temperature  $T_e$
- crystallographic order

Local order parameter for two different crystal volumes as a function of time after the impact of a 5-keV Ag atom onto an Ag(111) model crystallite. The right boundary plane is located at  $x=0$  Angstrom.

## Model Equations

### Excitation Energy Density $E(\vec{r}, t) \leftrightarrow T_e(\vec{r}, t)$

particle dynamics (MD)

$$M \frac{d^2 \vec{r}_i(t)}{dt^2} + \vec{K} \frac{d \vec{r}_i(t)}{dt} = -\nabla_{\vec{r}_i} V(\vec{r}_1(t), \vec{r}_2(t), \dots, \vec{r}_N(t))$$

electronic system

$$\frac{\partial E(\vec{r}, t)}{\partial t} - \nabla \cdot (D(T_l(\vec{r}, t), T_e(\vec{r}, t), \Lambda(\vec{r}, t)) \nabla E(\vec{r}, t)) = A \sum_{i=1}^N E_i^e(\vec{r}_i, t) \cdot \delta(\vec{r}_i - \vec{r}) + \sum_{i=1}^N E_{eh}(\vec{r}_i, t) - E_F \cdot \delta(t - t_{e0}^i) \cdot \delta(\vec{r} - \vec{r}_{e0}^i)$$

diffusion coefficient

$$D(\vec{r}, t) = \frac{1}{1 - \sqrt{N} \sqrt{f}} \left\{ D_0(\vec{r}, t) \left[ \Lambda(\vec{r}, t) - 1/\sqrt{N} \sqrt{f} \right] + D_{em} \left[ \Lambda(\vec{r}, t) \right] \right\}$$

$$\Lambda(\vec{r}, t) = \frac{1}{3N} \left| \sum_{j=1}^3 \cos \left( \frac{2\pi}{a_j} \sigma_j(\vec{r}, t) \right) \right|$$

$$D_0(\vec{r}, t) = \frac{1}{3} a T_e^2(\vec{r}, t) + b T_l(\vec{r}, t)$$

## Boundary Conditions

#### • Neumann conditions at the surface

- pseudo-infinite boundary conditions at other boundary planes (Green's functions method)
- crater formation dynamics treated as a moving boundary value problem

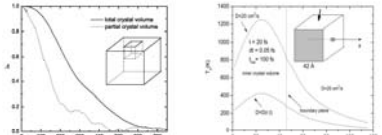
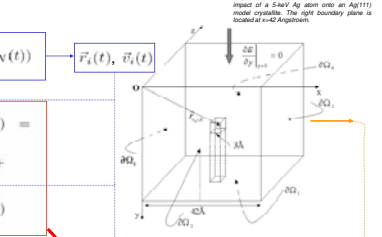


Fig. 4: Electron temperature along the central x-axis of the simulation volume 20 fs after the impact of a 5-keV Ag atom onto an Ag(111) model crystallite. The right boundary plane is located at  $x=0$  Angstrom.



$$I_m := \{(i, j, k) | \vec{r}_{i,j,k} \in \partial \Omega_m\}$$

$$\Delta E^{out,n} = \frac{1}{\Delta t} D_{out} \nabla E \cdot \vec{n}_{in} \Delta t$$

$$E(\vec{r}_{i,j,k} \in \partial \Omega_m, t_n) = \sum_{\alpha=0}^n \sum_{\beta=0}^n \sum_{\gamma=0}^n \Delta E_{\alpha,\beta,\gamma}^{i,j,k}$$

$$\times \frac{1}{(4\pi D_{out} (t_n - t_\alpha))^{\frac{3}{2}}} \exp \left( -\frac{|\vec{r}_{i,j,k} - \vec{r}_{j,k,\alpha}|^2}{4D_{out} (t_n - t_\alpha)} \right)$$

## Results

### Electron Promotion

- At which interatomic distance does the resonant electronic transition occur?

#### Stochastic Landau-Zener (LZ) approach

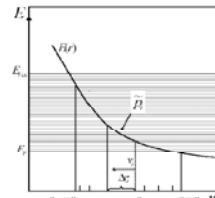


Fig. 5: Schematic drawing of the quasi-MO intersecting the conduction band.

- avoided crossings between MO diabatic energy curve and continuum states (Fig. 5)
- LZ transition probability given by

$$P_{ij} = \left[ 1 - \exp \left( -\frac{2\pi P_{ij}^2}{\hbar v |\Delta E_{ij}|} \right) \right]$$

- probability for transition at  $t_i$  is then

$$P_i = \frac{1}{N} \left[ 1 - \exp \left( -\frac{2\pi P_{ij}^2}{\hbar v |\Delta E_{ij}|} \right) \right] \times \Delta t \frac{dE}{dt} \times \prod_{k=1}^{i-1} (1 - P_k)$$

- Normalization factor  $N$  determined by the condition that, at the latest, the transition must occur at the turning point

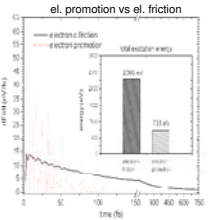


Fig. 6: Volume-integrated source terms (solid line) and electronic friction (dashed line) as a function of time after the projectile impact. Inset shows the total excitation energy generated within the first 250 fs after the initiation of the cascade.

#### Constant Rate Model

##### 5-keV Ag → Ag (111)

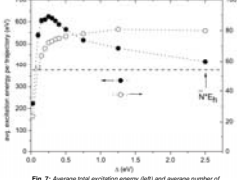


Fig. 7: Average total excitation energy (left) and average number of hot electrons (right) per trajectory for different level widths.

- Overlap of diabatic MO with conduction band states
- Virtual bound state (VBS) of finite width  $\Delta$
- transition rate given by Fermi's Golden Rule

$$\Gamma(E) = \frac{2\pi}{\hbar} |V_{\alpha}(E)|^2 \rho(E)$$

- approximation: constant transition rate  $\Gamma$  taken from experimental line widths  $\Delta$
- Monte-Carlo treatment of transitions within molecular dynamics code

##### excitation spectrum

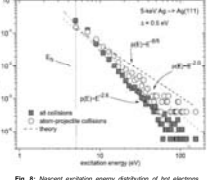


Fig. 8: Nearest excitation energy distribution of hot electrons generated in electron promotion events. Data taken from a set of 120 trajectories.

## Statistical Analysis of Energy Transfer Processes

#### • particle bombardment of solid surfaces is stochastic process

- averaging over large number of impact points
- comparison of average electron temperatures with temperatures obtained from high action events (Fig. 9)
- investigation of crystallographic effects (Fig. 10)

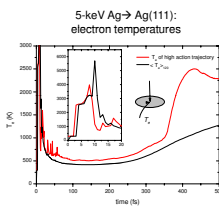


Fig. 9: Comparison of the electron temperatures of a high action trajectory ( $T_e = 20$ ) with electron temperature averaged over 120 trajectories ( $T_e = 10$ ).

##### Crystallographic effects

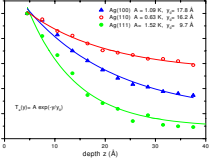


Fig. 10: Temperature depth profiles for different crystal orientation.

## Secondary Ion Formation in Sputtering

##### 5-keV Ag → Ag(111) ionization probabilities

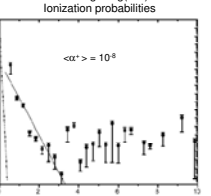
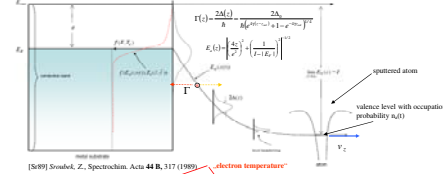


Fig. 11: Calculated ionization probabilities of sputtered atoms for 5-keV Ag → Ag(111) bombardment.

## Kinetic Electron Emission

#### • thermodynamical free-electron model

- numerical integration of Richardson-Dushman equation using the time- and space dependent electron temperature distribution at the surface

$$j_e(\vec{r}, t) = \frac{e m}{2\pi^2} (k_B T_e(\vec{r}, t))^{\frac{3}{2}} \times \sum_{i=1}^N (1 - \exp(-\frac{E_i(\vec{r}, t)}{k_B T_e(\vec{r}, t)}))$$

$$\gamma_{KEE} = \frac{1}{e n_0} \int_0^{\infty} \int_{\Omega} j_e(\vec{r}, t) dA dt$$

→ kinetic electron emission yield  $\gamma$  per trajectory

- averaging over many trajectories (Fig. 12)

#### Kinetic electron emission yields

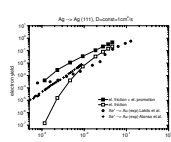


Fig. 12: Kinetic electron emission yield  $\gamma$  as a function of bombardment energy.  $\gamma$  has been averaged over 1200 trajectories. The total simulated time per impact was 50 fs.

## Selected Publications

- [1] Computer simulation of low-energy electronic excitation in atomic collision cascades. A. Duvenbeck, S. Srodek, Z. Srodek and A. Wucher. *Nucl. Instr. Meth. B* **228** (2004) 664-677
- [2] Self sputtering yields of silver under bombardment with polyatomic projectiles. A. Duvenbeck, M. Lindner and A. Wucher. *Nucl. Instr. Meth. B* **228** (2005) 170-175
- [3] Electronic excitation in atomic collision cascades. A. Duvenbeck, Z. Srodek and A. Wucher. *Nucl. Instr. Meth. B* **228** (2005) 325-329
- [4] Low energy electronic excitation in atomic collision cascades: a nonlinear transport model. A. Duvenbeck and A. Wucher. *Phys. Rev. B* **72** (2005) 165408
- [5] On the role of electronic friction and electron promotion in kinetic excitation of solids. A. Duvenbeck, O. Weingart, V. Bus and A. Wucher. *Nucl. Instr. Meth. B* **255** (2007) 281
- [6] The role of electronic friction of low-energy recoils in atomic collision cascades. A. Duvenbeck, O. Weingart, V. Bus and A. Wucher. *Nucl. Instr. Meth. B* **258** (2007) 83
- [7] Electronic friction and electron promotion in atomic collision cascades. A. Duvenbeck, O. Weingart, V. Bus and A. Wucher. *New J. Phys.* **9** (2007) 38
- [8] Modeling hot electron generation induced by electron promotion in atomic collision cascades in metals. A. Duvenbeck, B. Weidtmann, O. Weingart and A. Wucher. *Phys. Rev. B* **77** (2008) 245444 (1-7)

##### 5-keV Ag → Ag (111)

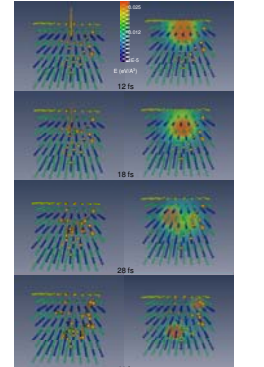


Fig. 13: Snapshots of one selected atomic collision cascade ( $\gamma = 0.50$ ) induced by 5-keV Ag → Ag(111) bombardment. The snapshots are taken 12, 18, 28 and 41 fs after the projectile impact onto the model crystal (720 atoms). Left: Evolution of the collision cascade in space and time. Atoms are enclosed (yellow, green, blue) according to the layer they originate from. Particles that are involved in close collisions in the course of the cascade are depicted in orange color. Right: In addition to the particle dynamics, the local excitation energy density is shown using the indicated color map.

- [9] Predicting secondary ion formation in MD simulations of sputtering. A. Duvenbeck, B. Weidtmann and A. Wucher. *Appl. Surf. Sci.* (2008) in press
- [10] Predicting kinetic electron emission in MD simulations of sputtering. A. Duvenbeck, B. Weidtmann and A. Wucher. *Nucl. Instr. Meth. B* (2008) submitted